Oxide ion conduction in La-doped PbWO$_4$ single crystals

Oxide ion conduction in La-doped PbWO$_4$ single crystals

Hongwei Huang[1]**, Xiqi Feng**[1]**, Wenliang Zhu**[1]**, Yan Zhang**[1]**,
Ting-Lian Wen**[1] **and Tong B Tang**[2]

[1] The State Key Laboratory of High Performance Ceramics and Superfine Microstructure,
Shanghai Institute of Ceramics, Chinese Academy of Sciences, Shanghai 200050, People's
Republic of China
[2] Physics Department, H K Baptist University, Waterloo Road, Kowloon, Hong Kong SAR,
People's Republic of China

E-mail: xqfeng@sunm.shcnc.ac.cn

Abstract
The effect of La dopant on the scintillating properties of lead tungstate has been
found to depend on the doping concentration. In this work the conductivities of
a series of PWO:La single crystals were measured and explained by a change
in doping mechanism. We propose that the oxygen vacancy is the main type of
charge carrier at all doping levels from room temperature to 1000 °C. Offering
high conductivity and low activation energy, heavily doped PWO:La may serve
as a fast ion conductor of merit.

1. Introduction

Oxide ionic conductors comprise an important class of functional materials and have been
studied for many years because of their applications as electrolytes in fuel cells, oxygen sensors,
films for oxygen separation and membrane reactors. Their main representatives known to date
possess fluorite and perovskite structures, with stabilized zirconia being the best known among
them.

Lead tungstate, i.e. PbWO$_4$ (or PWO for brevity), is also expected to be a good ionic
conductor in view of its tetragonal scheelite-type symmetry, which can be derived from
the fluorite-type structure given that Pb and W, which have similar electro-negativities, are
equivalent. Although Groenink and Binsma did not obtain significant conductivities in
Czochralski-grown single crystals [1], higher values were found in La- and Sm-doped ceramic
samples [2, 3]. In this work, we have examined La-doped single crystals with different doping
levels at elevated temperatures and compared the results with our previously reported data for
low temperatures [4].

An important reason for focusing our attention on monocrystalline PWO:La relates to its application as a scintillating material in high-energy particle detectors [5, 6]. La at low concentration (several hundred ppm) leads to dramatic improvements in its optical transmittance, decay time and radiation hardness [5]. However, with a further increase in concentration different effects appear [7]. This implies a transformation of the doping mechanism, which should also manifest itself as a change in electrical conductivity. To derive more detailed information on the lattice environment of the dopant, we have also performed x-ray photoelectron spectroscopic (XPS) experiments.

2. Experiment

Three La-doped PWO single crystals were grown from 5N powders. One was grown via the improved Bridgman method, with a nominal impurity molar concentration of 100 ppm (as calculated from a segregation constant of $k = 2.5$). The other two were grown using the Czochralski method with La levels in the melt of 1 and 2.5 mol%, respectively. All samples were cut into about $10 \times 10 \times 1$ mm^3, with their large faces perpendicular to the c-axis. Platinum was sputtered onto those large faces to create electrodes. An electrochemical work-station (model IM6e from Zahner) served for the measurement of ac conductivity, in air, at 50 °C intervals over the temperature range 680–1000 °C, with an ac voltage of 200 mV in amplitude.

XPS was carried out in a Micro-Lab 310-F (from VG Scientific) on samples that had been freshly cut into plates of about $10 \times 10 \times 2$ mm^3. Spectra at a single photon energy were recorded using Al Kα radiation, a hemispherical photoelectron energy analyser and a multi-channel electron detector.

3. Results and discussions

3.1. Low-temperature conductivity

From room temperature to 320 °C, ac conductivities are available from an earlier impedance spectroscopic study [4] on the dielectric properties of PWO:La crystals (of 100 ppm, 1 and 2.5 mol%). The data follow Jonscher's power law [8]:

$$\sigma_{\text{tot}}(\omega) = \sigma_{\text{dc}} + A\omega^s, \tag{1}$$

where σ_{dc} is the frequency-independent conductivity, A is a temperature-dependent parameter, and s is a constant between 0 and 1. The second term is a purely dispersive component of the conductivity that depends on the measurement frequency ω in a characteristic power-law fashion. This characteristic has been seen in a wide range of ionic conductors, especially in 'fast' ionic conductors which possess relatively high ionic mobilities [9]. Figure 1 presents a representative set of data.

Bulk dc resistances can be determined from the real-axis intercept of low-frequency arcs in the complex plane plots. The dc conductivities, σ, calculated in this way have been analysed with the help of the Arrhenius relation in the form $\sigma = \sigma_0 \exp(-E_a/\kappa T)$, where σ_0 denotes the pre-exponential factor and E_a denotes the activation energy for ionic migration. The temperature dependence of σ shows a good fit for all samples (see figure 2).

Activation energies were calculated from both impedance and electric modulus spectroscopies. Results close to 0.78 eV were found for all La-doped crystals, implying the same ionic-hoping mechanism for transport [10].
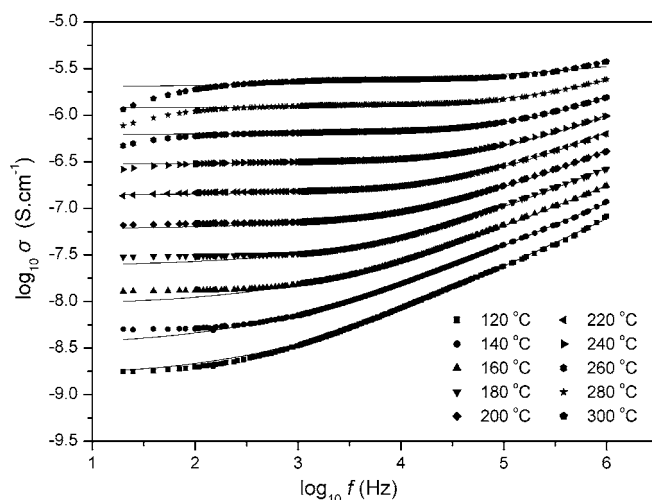
Figure 1. The frequency dependence of the ac conductivity at different temperatures for 2.5 mol% PWO:La. The solid curves are fitted to data points.
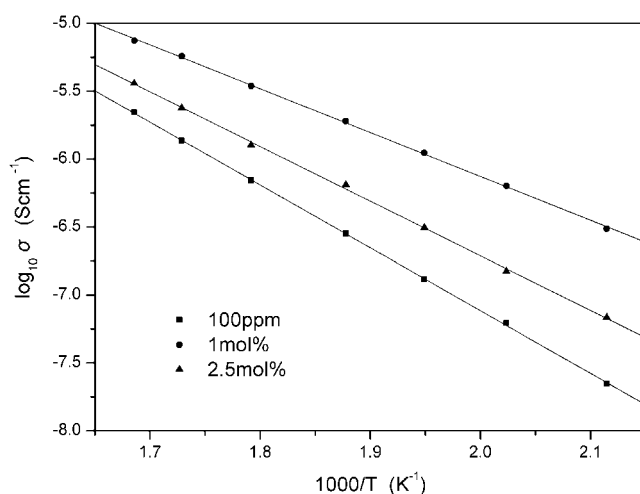

Figure 2. The temperature dependence of σ at low temperatures. The solid lines represent least-squares fits.

3.2. High-temperature conductivity

Arrhenius plots of the conductivities at 1 kHz, measured with the electrochemical workstation in this work, are also linear, as shown in figure 3. Table 1 lists the activation energies obtained, as well as those for the low-temperature cases discussed previously.

The high-temperature conductivity increases significantly with the rise in dopant level. It reaches 1.6×10^{-2} S cm^{-1} at 997 °C for 1 mol% and 2.8×10^{-2} S cm^{-1} at 957 °C for 2.5 mol% doping, about two orders of magnitude greater than that for the 100 ppm sample.
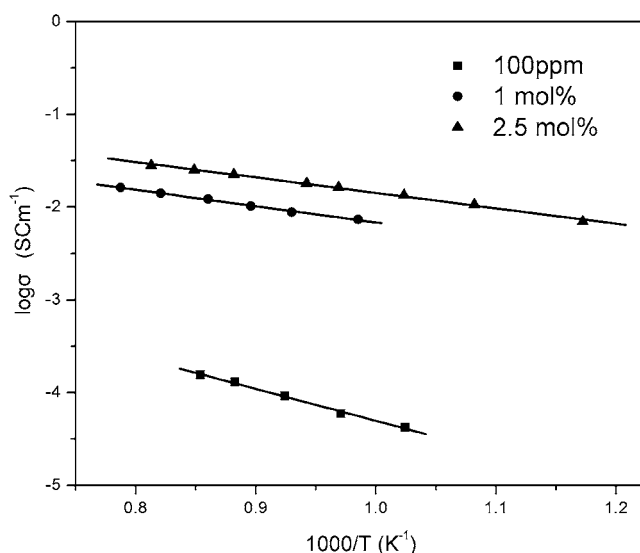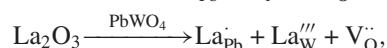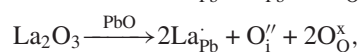
Figure 3. The temperature dependence of conductivity at 1 kHz at high temperatures, with least-squares fits shown by solid lines.

Table 1. The activation energies for conduction in La-doped PWO (LT—low-temperature region, from [4]; HT—high-temperature region).

La concentration	Activation energy, E (eV)		
	LT (E_a)	LT (E_{fp})	HT
100 ppm	0.76	0.77	0.68
1 mol%	0.78	0.79	0.35
2.5 mol%	0.80	0.79	0.33

3.3. La ion doping mechanism

There are mainly three possible mechanisms for La^{3+} doping [4]:

$$La_2O_3 \xrightarrow{PbO} 2La_{Pb}^{\cdot} + V_{Pb}'' + 3O_O^x,$$

$$La_2O_3 \xrightarrow{PbO} 2La_{Pb}^{\cdot} + O_i'' + 2O_O^x,$$

$$La_2O_3 \xrightarrow{PbWO_4} La_{Pb}^{\cdot} + La_W''' + V_O^{\cdot\cdot},$$

where $PbWO_4$ represents the bulk crystal. Computer simulation following the Mott–Littleton method [11] suggests that the first process, i.e. substitution at Pb sites with charge compensation by lead vacancies, is energetically most favoured. The least favoured is the last, according to which La ions enter the W sublattice.

An experimental check was instituted with the help of XPS. As figure 4 shows, whereas the spectrum from PWO:La (100 ppm) exhibits no features, two peaks at 836 and 853 eV are clearly present in the 1.0 or 2.5 mol% cases, and attributable to the orbitals La $3d_{5/2}$ and La $3d_{3/2}$, respectively. Each peak can be resolved as a superposition of two Gaussian components. As argued in a previous work that was based on extended x-ray absorption fine structure (EXAFS) measurements [11], the split of the peaks arises from the additional occupancy of La^{3+} at W sites.
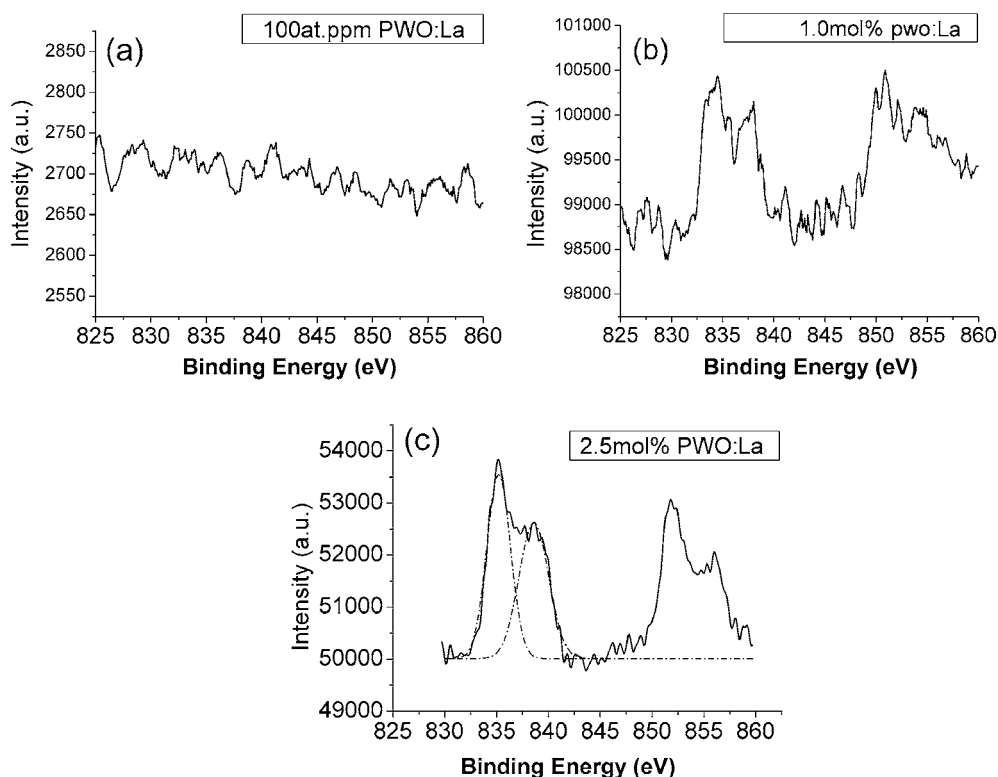
Figure 4. XPS spectra of PWO doped with La to (a) 100 at. ppm, (b) 1.0 mol% and (c) 2.5 mol%, fitted by Gaussian curves (the dashed curves).

It should be noted that heavy doping of La does not change the crystal structure or induce a new phase in PWO [12]. Also, different crystal growth methods (whether improved Bridgman or Czochralski) have no discernible effect on its conductivity properties [4].

Before discussing our single-crystal results, we should first review the work on PWO:La ceramics by Esaka *et al* [2], who examined two varieties of the doped material, of nominal compositions $Pb_{1-x}La_xWO_{4+x/2}$ and $Pb_{1-x}La_{2x/3}WO_4$, respectively. The authors made EMF measurements using an oxygen gas concentration cell with either as the electrolyte and affirmed the oxygen ion transport number to be approximately unity in both cases, indicating the oxide ion as the main charge carrier. In $Pb_{1-x}La_xWO_{4+x/2}$ ($x = 0.2$) they obtained a conductivity of 4.2×10^{-2} S cm^{-1} at 800 °C. According to the authors, for La^{3+} ions substituted at Pb^{2+} sites, charge neutrality was maintained by the creation of half the number of interstitial oxide ions, and the latter species was responsible for conduction. In $Pb_{1-x}La_{2x/3}WO_4$, charge compensation was by cation vacancies rather than oxygen interstitials. Nevertheless, the conductivity they measured for $x = 0.10$ reached 1.9×10^{-2} S cm^{-1} at 800 °C, the same order of magnitude as for the interstitial-rich system.

Let us make a more quantitative analysis of the discrepancy. As is well known, the electrical conductivity contributed by a single species is

$$\sigma = nq\mu, \tag{2}$$

where n, q and μ denote species concentration, charge and mobility, respectively. Since the conductivity activation energy is 0.59 eV for $Pb_{0.8}La_{0.2}WO_{4.1}$ and 0.38 eV for $Pb_{0.9}La_{2/30}WO_4$

in the high-temperature range [2], the ratio of their charge carrier concentrations turns out to be

$$R \approx \frac{4.8 \times 10^{-2}}{1.9 \times 10^{-2}} \frac{\exp(-\frac{0.38}{\kappa \times 1073})}{\exp(-\frac{0.59}{\kappa \times 1073})} \approx 25. \tag{3}$$

If the carriers are identified as interstitial oxygen ions, the difference in concentrations is far smaller than that expected from stoichiometric considerations. Given the earlier deduction from EMF data that the charge carriers are oxide ions, if they cannot be interstitials then they must be oxygen vacancies.

As proposed in [4], oxygen interstitials exist in PWO with heavy doping levels such as 1 and 2.5 mol%, but for such samples the concentrations of intrinsic Pb vacancies and oxygen interstitials are insufficient to fulfill charge balancing. A self-compensation mechanism has been suggested, in which La ions substitute at both Pb and W sites, leading to oxygen vacancies. The splitting of XPS peaks offers support to this additional occupancy of W sites. Charge association complexes $[(La_W)^{3-}-(La_{Pb})^{\cdot}-V_O^{\cdot\cdot}]$ produced in this mechanism may explain the observed superstructure [13] or act as killing sites in the luminescence decay process [7]. A similar mechanism has been reported in Cr^{3+}-doped $LiNbO_3$ single crystals [14].

In the high-temperature region the conductivities of our three crystals increase with dopant concentration. However, their doping levels have not reached those of PWO:La ceramics [2], in which the conductivity has been observed to increase with lanthanum content at first, and then decrease. In other materials, such as doped CeO_2 [15], the occurrence of such conductivity maxima has been studied extensively and ascribed to the formation of defect clusters, namely $[2Y'_{Ce}-V_O^{\cdot\cdot}]$ in the cited case. At low temperatures extensive dopant–vacancy clustering occurs and the Arrhenius energy had a substantial contribution from the energy required to dissociate the cluster. At higher temperatures the vacancies are already partially or completely dissociated, and the conductivity Arrhenius energy approaches the hopping activation energy of vacancies.

As for our PWO:La, as doping rises, cation vacancies V_{Pb}, oxygen interstitials and La at W sites form gradually, until heavy doping produces the clusters $[(La_W)^{3-}-(La_{Pb})^{\cdot}-V_O^{\cdot\cdot}]$ that are responsible for the conductivity maximum. At high temperatures, oxygen vacancies dissociate from the clusters and take part in conduction. This explains why the conductivity of 1 mol% La-doped crystal exceeds that of the 2.5 mol% sample at low temperature but becomes smaller at high temperature. It also shows that the oxygen vacancy is the main carrier for different doping levels over the full range of temperature measurements. The high-temperature activation energy for the 100 ppm sample is similar to that for crystals of all doping levels in the low-temperature region. However, the high-temperature activation energies in the 1 and 2.5 mol% cases are both only about 0.33 eV.

The low activation energy and high conductivity of PWO:La have drawn our attention to its potential application as fast ion conductors, and in table 2 we compare it with ZrO_2 and CeO_2, which are tetravalent oxides with fluorite structures that have been widely utilized as such. Its merits include chemical stability, low cost and the possibility for higher conductivity with optimum doping.

4. Conclusion

The oxygen vacancy is the main type of charge carrier for conduction in PWO:La. Heavy doping causes La ions to occupy W^{6+} sites and $[(La_W)^{3-}-(La_{Pb})^{\cdot}-V_O^{\cdot\cdot}]$ clusters to form. Heavily doped La:PWO can be a potential oxide ion conductor at high temperatures.

Table 2. The conductivities and activation energies of representative fluorite-structure oxides and of PWO:La. (Data for ThO$_2$, ZrO$_2$ and CeO$_2$ are taken from [16].)

Crystal	Conductivity (S cm^{-1}) (1000 °C)	Activation energy (eV)
ThO$_2$ + 8% Y$_2$O$_3$	0.0048	1.1
ThO$_2$ + 5% CaO	0.000 47	1.1
ZrO$_2$ + 12 mol% CaO	0.055	1.1
ZrO$_2$ + 9 mol% Y$_2$O$_3$	0.12	0.8
ZrO$_2$ + 10 mol% Sm$_2$O$_3$	0.058	0.95
ZrO$_2$ + 8 mol% Yb$_2$O$_3$	0.088	0.75
ZrO$_2$ + 10 mol% Sc$_2$O$_3$	0.25	0.65
CeO$_2$ + 11 mol% La$_2$O$_3$	0.08	0.91
CeO$_2$ + 15 mol% CaO	0.025	0.75
PWO:La (1 mol%)	0.016	0.35
PWO:La (2.5 mol%)	0.028 (957 °C)	0.33

Acknowledgments

References

[1] Groenink J A and Binsma H 1979 *J. Solid State Chem.* **29** 227
[2] Esaka T, Mina-ai T and Iwahara H 1992 *Solid State Ion.* **57** 319
[3] Esaka T, Tachibana R and Takai S 1996 *Solid State Ion.* **92** 129
[4] Huang H W, Feng X Q, Man Z Y, Tang T B, Dong M and Ye Z G 2003 *J. Appl. Phys.* **93** 421
[5] Kobayashi M, Usuki Y, Ishii M, Yazawa T, Hara K, Tanaka M, Nikl M and Nitsch K 1997 *Nucl. Instrum. Methods Phys. Res.* A **399** 261
[6] Kobayashi M *et al* 2001 *Nucl. Instrum. Methods Phys. Res.* A **459** 482
[7] Nikl M, Bohacek P, Nitsch K, Mihokova E, Martini M, Vedda A, Croci S, Pazzi G P, Fabeni P, Baccaro S, Borgia B, Dafinei I, Diemoz M, Organtini G, Auffray E, Lecoq P, Kobayashi M, Ishii M and Usuki Y 1997 *Appl. Phys. Lett.* **71** 3755
[8] Jonscher A K 1981 *J. Mater. Sci.* **16** 2037
[9] Almond D P 1983 *Solid State Ion.* **8** 159
[10] Reau J M, Jun X, Senegas J, Deit Ch Le and Poulain M 1997 *Solid State Ion.* **95** 191
[11] Zhu W L, Feng X Q, Huang Y L, Lin Q S and Wu Z H 2002 *Phys. Status Solidi* a **193** 211
[12] Lin Q, Feng X, Man Z and Shi C 2001 *Chin. J. Struct. Chem.* **20** 214
[13] Lin Q and Feng X 2001 *Ferroelectrics* **251** 85
[14] Park I W, Choh S H, Song K J and Kim J N 1993 *J. Korean Phys. Soc.* **26** 173
[15] Riess I 1989 *Science and Technology of Fast Ion Conductors* ed H L Tuller and M Balkanshki (New York: Plenum) p 23
[16] Lin Z X, Guo Z K, Sun C W, Li S C, Chen K G, Tian S B and Yan D S 1979 *Fast Ion Conductor (Solid Electrolyte)* (Shanghai: Shanghai Science and Technology Press)